Rendering Iridescence in Multilayer Structures

Dakota Erskine
Rensselaer Polytechnic Institute
New York, USA
erskid@rpi.edu

Christopher Poon
Rensselaer Polytechnic Institute
New York, USA
poonc3@rpi.edu

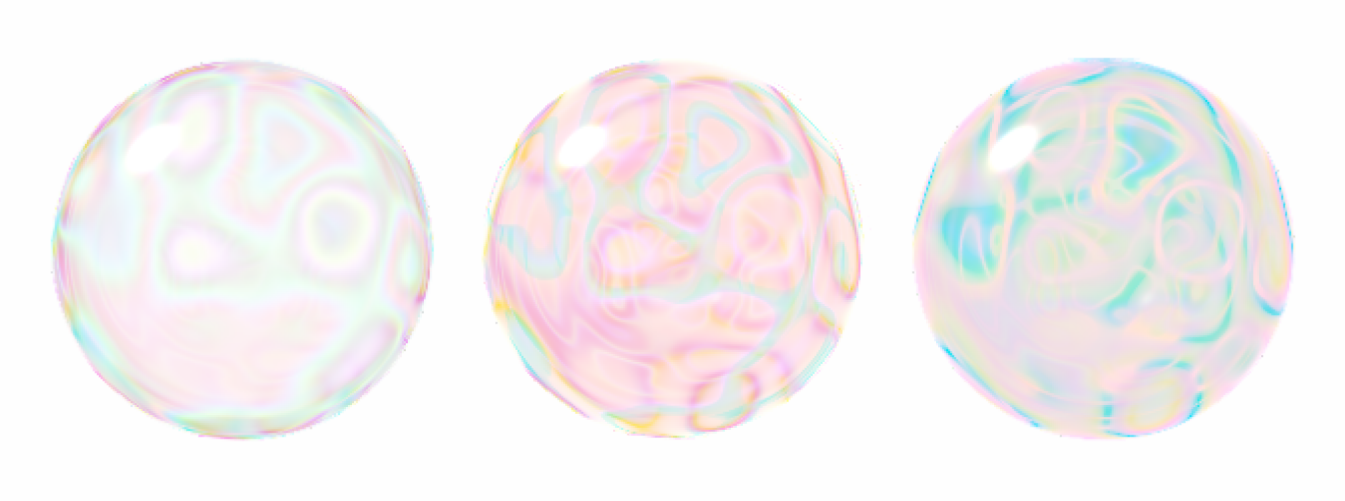

Figure 1: Various renderings of soap bubbles.

Abstract

We present a physically-based method for rendering iridescence caused by thin-film interference in multilayer structures. Unlike previous approaches that rely on precomputed textures or single-layer approximations, our model implements the full transfer matrix method to accurately simulate the interaction of light with stacks of arbitrarily many layers. Our computed results demonstrate the efficacy of our approach in reproducing complex interference effects, such as angle-dependent color shifts, layered patternation, and absorption. We additionally consider the use of spectral sampling to more precisely capture shifts in color, as well as procedural noise to model variations in film thickness.

CCS Concepts

• **Computing methodologies** → **Reflectance modeling**.

Keywords

rendering, iridescence, thin-film interference, multilayer, transfer matrix method

1 Introduction

Iridescence, also known as goniochromism, is an optical phenomenon inherent in thin films and layered materials whereby surface coloration appears to shift with the angle at which it is viewed. This effect is commonly observed in soap bubbles, oil slicks, and insect wings and occurs due to the interference of light as it reflects and transmits through a stack of films. Accurately capturing the nuances of this effect is essential for realistically rendering the appearances of many natural and synthetic materials.

Although iridescence has been studied extensively in both optics and computer graphics, most rendering approaches simplify the underlying physics to achieve practical performance. Common methods often involve analytical approximations based on single-layer interference. While these techniques can produce visually plausible results, they are often limited in their ability to capture the full range of optical phenomena demonstrated by multilayer structures. Moreover, these simplifications can lead to inaccuracies in reflected intensities and color variations.

In this paper, we develop a method for rendering iridescence that directly models the interference of light within multilayer thin films using the transfer matrix method. Our approach supports arbitrary layer counts, complex-valued refractive indices, and polarization-dependent interactions, making it particularly suited to the task of rendering materials that exhibit this effect. To compute wavelength-dependent reflectances, we employ spectral sampling, ensuring physically plausible shifts in color under varying illumination and viewing conditions. Additionally, we incorporate procedural noise to represent spatial variations in film thickness, allowing for naturalistic interference patterns across a surface.

2 Background

Various techniques have been proposed to address the problem of rendering iridescence, ranging from wave interference models to microfacet-based approximations. Early foundational work by Gondek et al. [4] introduced the concept of wavelength-dependent

reflectance models, demonstrating the importance of accounting for spectral variations when simulating interference-based effects. Building upon this foundation, Hirayama et al. [5] proposed an illumination model for multilayer films that explicitly incorporates light interactions and phase shifts at each interface, enabling the rendering of interference patterns arising from complex layered structures.

To simulate spatially-varying iridescence in biological structures such as butterfly wings, Wu and Zheng [9] combined microfacet-based models with multi-beam interference equations. Belcour and Barla [2] further extended microfacet theory with an approximation of interference effects. Their model captures angle-dependent color shifts by directly modifying the reflectance term of the BRDF, allowing for real-time rendering of thin-film interference on rough surfaces.

More recent developments have emphasized the accuracy of the computed results. Benamira and Pattanaik [3] applied the transfer matrix method to realistically render anti-reflective coatings, providing a rigorous framework for modeling multilayer interference. Similarly, Hurben [6] and Oton [7] explored practical implementations of the transfer matrix method to capture the optical behavior of layered media. These recent developments reflect a growing interest in the transfer matrix method as a more precise model to describe multilayer interference.

Our work builds upon this interest by directly applying the transfer matrix method to simulate iridescence in layered materials, extending beyond anti-reflective coatings to more general structures with varying refractive indices and thicknesses. By adopting a physically-based approach, we aim to capture the complex interference patterns that arise from the interaction of light with layered structures across a broad range of materials.

3 Motivation

Microfacet theory underlies many physically-based approaches to rendering effects at the nanoscale level. Rather than assume a perfectly smooth surface, we model objects as collections of microscopic planar facets, or microfacets, each reflecting and transmitting light independently. These interactions are then aggregated into a single term that captures the overall reflectance of the system, allowing us to simulate the complex and intricate behavior of light that arises from surface microstructure.

Each microfacet interacts with light according to the Fresnel equations, which describe the reflection and transmission of light at an interface between two media. For s- and p-polarized light, the respective coefficients are

$$r_s = \frac{n_1 \cos\theta_i - n_2 \cos\theta_t}{n_1 \cos\theta_i + n_2 \cos\theta_t} \tag{1}$$

$$r_p = \frac{n_2 \cos\theta_i - n_1 \cos\theta_t}{n_2 \cos\theta_i + n_1 \cos\theta_t} \tag{2}$$

$$t_s = \frac{2n_1 \cos\theta_i}{n_1 \cos\theta_i + n_2 \cos\theta_t} \tag{3}$$

$$t_p = \frac{2n_1 \cos\theta_i}{n_2 \cos\theta_i + n_1 \cos\theta_t} \tag{4}$$

Here, n_1 is the refractive index of the first medium, n_2 is the refractive index of the second medium, θ_i is the incident angle, and

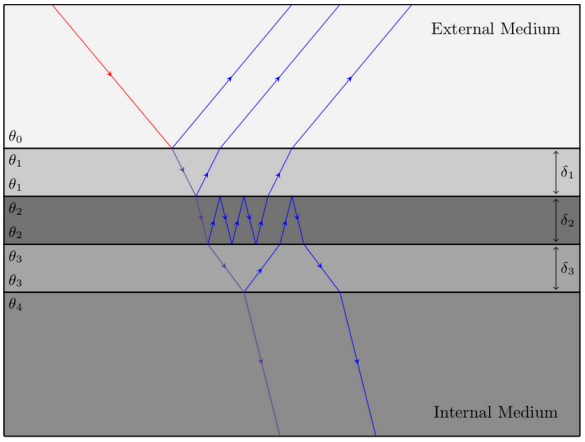

Figure 2: An incident ray (red) comes into contact with the first interface, where it partially reflects (blue) away from and partially transmits (purple) into the next medium. At each interface, light undergoes more reflections and transmissions, generating multiple internal paths [1].

θ_t is the transmitted angle. The two angles are related via Snell's law:

$$n_1 \sin\theta_i = n_2 \sin\theta_t \tag{5}$$

In what follows, we simplify notation by using r_{ij} and t_{ij} to denote the reflection and transmission coefficients between media i and j. Furthermore, we assume unpolarized light.

These interface-level reflection and transmission coefficients serve as the foundational elements for computing how light propagates through layered structures. As illustrated in Figure 2, light within a stack of thin films undergoes multiple internal reflections and transmissions, accumulating phase differences at each intersection. These phase shifts result in wavelength-dependent interference, producing iridescence.

To accurately model this behavior, we must compute the total reflectance R and transmittance T of the system. These quantities encapsulate the cumulative effect of all interface interactions, including amplitude changes and phase shifts.

4 The Transfer Matrix Method

To compute interference effects across multilayer thin films, we adopt the transfer matrix method—a standard technique in optics that models how light reflects and transmits within layered media. Grounded in electromagnetic theory, this method captures the full complexity of thin-film interference, including any absorption within lossy materials, by accounting for both amplitude and phase changes at each interface and within each medium.

In this formulation, every interface between adjacent media is described by an interface matrix that encapsulates reflection and transmission coefficients, and every medium of finite thickness is associated with a propagation matrix that accounts for phase shifts. As illustrated in Figure 3, the electric field within any layer consists of both forward- and backward-propagating waves. The transfer matrices relate these waves across the entire structure.

Each interface introduces new reflections and transmissions. To accurately capture this behavior, we relate the wave amplitudes across two media with the corresponding interface matrix. For a single interface between media i and j, this relation is written as

$$\begin{bmatrix} E_i^+ \\ E_i^- \end{bmatrix} = \underbrace{\frac{1}{t_{ij}} \begin{bmatrix} 1 & r_{ij} \\ r_{ij} & 1 \end{bmatrix}}_{\mathcal{D}_{ij}} \begin{bmatrix} E_j^+ \\ E_j^- \end{bmatrix} \tag{6}$$

The terms E_i^+ and E_i^- indicate the forward- and backward-propagating wave amplitudes in medium i, and $\mathcal{D}_{ij}$ denotes the matrix corresponding to an interface between media i and j.

Light propagating within a uniform layer accumulates a phase shift without changing direction. This is illustrated in Figure 4, which shows how the wave components traverse a uniform medium. We encapsulate this behavior with $\mathcal{P}_j$, the propagation matrix corresponding to medium j, by writing

$$\begin{bmatrix} E_j^+ \\ E_j^- \end{bmatrix} \leftarrow \underbrace{\begin{bmatrix} e^{-i\phi_j} & 0 \\ 0 & e^{i\phi_j} \end{bmatrix}}_{\mathcal{P}_j} \begin{bmatrix} E_j^+ \\ E_j^- \end{bmatrix} \tag{7}$$

$$\phi_j = \frac{2\pi n_j d_j}{\lambda} \cos\theta_j \tag{8}$$

In this expression, d_j is the width of medium j, n_j the refractive index of medium j, λ the wavelength of the incident light, and θ_j the internal angle of incidence.

A single thin film is modeled as a stack consisting of an interface, followed by a propagation region, followed by another interface. An example of this structure is shown schematically in Figure 5. The corresponding matrices are accordingly composed left-to-right and the relation given as

$$\begin{bmatrix} E_0^+ \\ E_0^- \end{bmatrix} = \mathcal{D}_{01}\mathcal{P}_1\mathcal{D}_{12} \begin{bmatrix} E_2^+ \\ E_2^- \end{bmatrix}$$

To evaluate the optical behavior of a complete, N-layer system, we compose all interface and propagation matrices into a single system matrix $\mathcal{M}$, which yields the more general relation

$$\begin{bmatrix} E_0^+ \\ E_0^- \end{bmatrix} = \underbrace{\mathcal{D}_{01}\mathcal{P}_1\mathcal{D}_{12}\mathcal{P}_2 \ldots \mathcal{P}_N\mathcal{D}_{N(N+1)}}_{\mathcal{M}} \begin{bmatrix} E_{N+1}^+ \\ E_{N+1}^- \end{bmatrix} \tag{9}$$

Finally, from the system matrix, we compute the total reflectance and transmittance of the system as

$$R = \left| \frac{\mathcal{M}_{12}}{\mathcal{M}_{11}} \right|^2 \tag{10}$$

$$T = \frac{n_{N+1}\cos\theta_{N+1}}{n_0\cos\theta_0} \left| \frac{1}{\mathcal{M}_{11}} \right|^2 \tag{11}$$

These quantities may alternatively be related through the law of conservation of energy, which implies $R + T = 1$.

Together, R and T capture the cumulative effect of all light interactions within the multilayer structure. This matrix formulation supports arbitrary layer counts and provides a physically-grounded foundation for simulating thin-film interference.

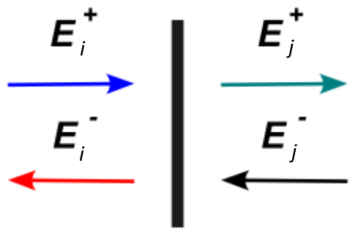

Figure 3: A system of forward- and backward-propagating waves on both sides of an interface. The green wave results from the transmission of the blue wave and the reflection of the black wave. Similarly, the red wave results from the transmission of the black wave and the reflection of the blue wave [6].

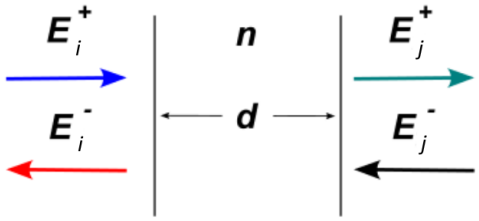

Figure 4: A system of forward- and backward-propagating waves on both sides of a medium with width d and refractive index n. The propagation of these waves within the medium introduces a phase shift [6].

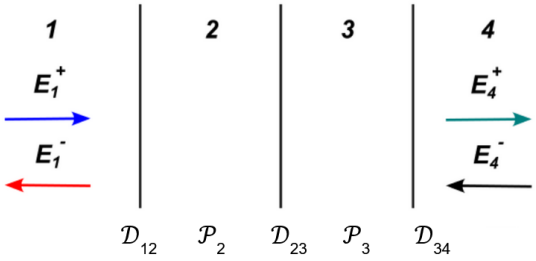

Figure 5: A system of forward- and backward-propagating waves across three interfaces and two finite-width media [6].

5 Spectral Sampling

For our initial implementation, we only sample reflectance at three wavelengths—650 nm (red), 510 nm (green), and 475 nm (blue)—and take these values as an RGB triple. Although this approach is efficient and easy to incorporate in RGB-based renderers, it fails to capture the subtle variations in color that arise from thin-film interference across the full visible spectrum. As a result, certain colors can appear lost or overrepresented, limiting the realism of the rendered iridescence.

To improve accuracy, we adopt a spectral sampling strategy, computing reflectance at uniform, integer-spaced wavelengths from 380 nm to 780 nm. We then integrate these results using the CIE

1931 color matching functions, weighting each sample by the D65 standard illuminant to simulate natural lighting conditions. We note that substitutions to either the color matching functions or the illuminant may be necessary to simulate different perceptual models or lighting conditions, but we have found that this combination produces suitable results for a variety of different cases.

The resolution of this strategy is determined by the number of discrete wavelengths sampled. In particular, an n-wavelength sampling yields a spacing of $\frac{400}{n-1}$ nm, allowing us to compute reflectance at regular intervals. This approach ensures consistent coverage of the visible spectrum and simplifies numerical integration with tabulated data. As n increases, the computed reflectance more accurately captures the fine-grained variations in color characteristic of interference phenomena.

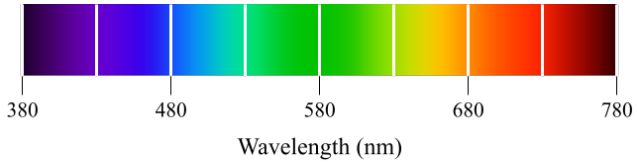

Figure 6: An example of spectral sampling at uniform wavelengths. With nine samples, reflectance is evaluated every 50 nm.

6 Procedural Film Thickness

Real-world thin-film structures often demonstrate irregularities in thickness, which give rise to complex patterns not captured by uniform-thickness models. We represent this variation procedurally by modulating the thickness of the film with Perlin noise [8], treating the noise value as a linear interpolation weight between the minimum and maximum thicknesses of the thin film. More precisely, the thickness at a point $\mathbf{p}$ is

$$d(\mathbf{p}) = d_{\text{min}} + (d_{\text{max}} - d_{\text{min}}) \cdot n(s \cdot \mathbf{p}) \tag{12}$$

Here, d_{min} is the minimum film thickness, d_{max} the maximum film thickness, n the noise function, and s a scalar controlling the frequency of the noise. We find that this formulation produces smooth, continuous variations in the computed reflectance. Additionally, it enables fine-grained control over the scale and intensity of these variations. Larger values of s produce more extreme gradations, while smaller values yield broader, more gradual changes.

7 Results

We implemented our multilayer thin-film interference model in C++ as part of a Whitted-style ray tracer and evaluated its performance on an AMD Ryzen 9 9900x CPU. To support complex-valued arithmetic as required by the transfer matrix method, we used the complex class from the C++ Standard Template Library and developed a custom ComplexMatrix class. All results were generated using this implementation with no hardware acceleration.

To assess the accuracy and efficiency of our model, we conducted tests across a range of configurations and conditions.

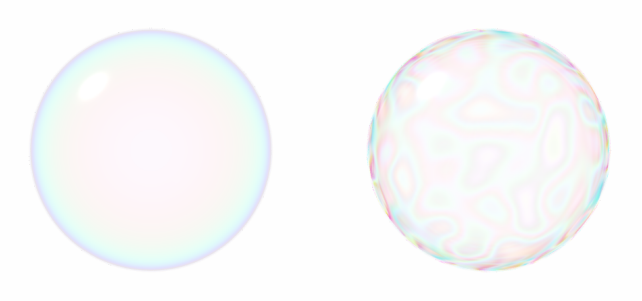

Figure 7: Soap bubbles rendered with uniform (left) and non-uniform (right) film thicknesses.

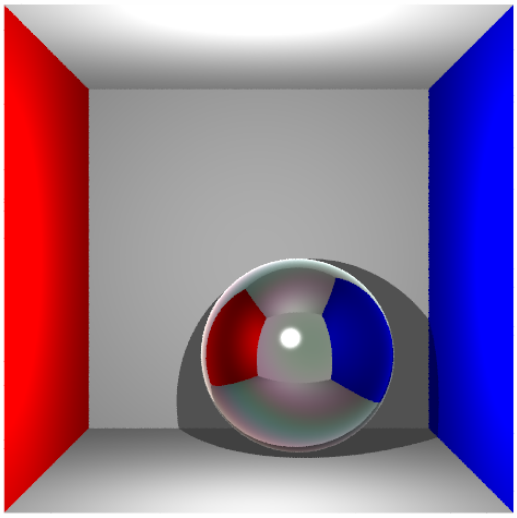

Figure 8: A reflective sphere rendered with a thin film with a refractive index of 1.5 + 0.15i, demonstrating the combined effect of absorption and iridescence.

These included stacks with varying numbers of layers, refractive indices, and thicknesses both uniform and procedurally generated. Our method successfully reproduced key features of thin-film interference—namely angle-dependent color shifts, layered interference patterns, and wavelength-selective absorption—across all cases.

The resulting renderings matched physical expectations, with noticeable shifts in hue caused by constructive and destructive interference. These effects were especially pronounced in film stacks with extreme contrasts in refractive index, as well as those with non-uniform thickness profiles. Spectral sampling further improved the realism of these results, eliminating artifacts caused by undersampling and revealing hues like violet and cyan that were previously lost.

As expected, rendering times increased linearly with both the number of layers and the number of wavelength samples. Despite this, our model remained computationally tractable across all tested cases. For instance, a scene with a 2-layer stack and procedural film

Figure 9: A negative imaginary term in the index of refraction yields an amplification effect, as can be seen in this rendering of an iridescent metal ring.

thickness was rendered with 41 wavelength samples at 500x500 resolution in approximately 7.2 minutes on a single thread.

These results demonstrate that the full transfer matrix approach is both physically accurate and practical for simulating multilayer thin-film interference. Its predictable overhead, compatibility with spectral rendering, and ability to handle arbitrary layer configurations make it a strong candidate for integration into existing offline rendering pipelines.

8 Conclusion

We have presented a physically-based framework for rendering iridescence caused by multilayer thin-film interference using the transfer matrix method. Our approach captures the cumulative effects of light propagation across a stack of thin films, enabling accurate simulation of wavelength- and angle-dependent color variation. In addition to phase-driven effects, the model also accounts for absorption from lossy materials, supporting both vibrant and muted interference effects with physical accuracy. By incorporating spectral sampling and procedural variations in film thickness, our method produces realistic and detailed interference patterns.

Looking ahead, several directions remain open for future work. While our current model focuses on smooth, planar surfaces, further integrating the transfer matrix framework with microfacet theory would allow for more realistic representations of iridescent materials under complex lighting and surface roughness conditions. Additional improvements could include supporting polarization-aware lighting effects, accounting for dispersion, and optimizing matrix evaluations for faster computation. Finally, more extensive validation against measured reflectance data could reinforce the physical accuracy of our results and guide future refinements to this approach.

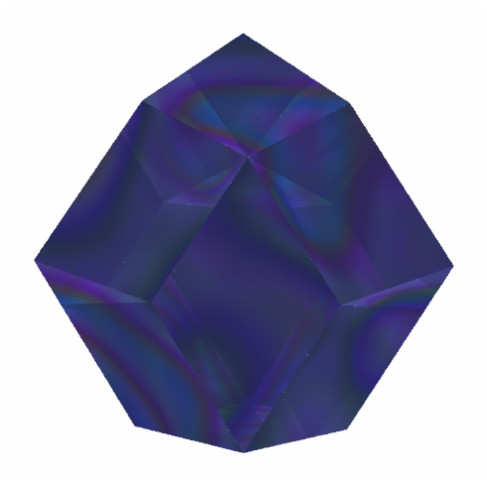

Figure 10: A rendering of a blue gem with a film of thickness 100-1000 nm, variation scalar 1, and index of refraction 1.76.

Acknowledgments

We would like to thank Dr. Barbara Cutler for her guidance and support throughout the semester, as well as for providing the base code upon which our implementation was built. We would also like to thank Bacterius, whose accessible guide informed aspects of our initial, single-layer implementation and helped shape our early understanding of the problem. Additionally, we would like to acknowledge Adrian Biagioli for his tutorial on Perlin noise, which provided helpful reference code for the thickness variation component of our project.

References

[1] Bacterius. 2013. Thin film interference for Computer Graphics. Retrieved April 16, 2025 from https://gamedev.net/tutorials/_/technical/graphics-programming-and-theory/thin-film-interference-for-computer-graphics-r2962/

[2] Laurent Belcour and Pascal Barla. 2017. A practical extension to microfacet theory for the modeling of varying iridescence. *ACM Trans. Graph.* 36, 4, Article 65 (July 2017), 14 pages. doi:10.1145/3072959.3073620

[3] Alexis Benamira and Sumanta Pattanaik. 2020. Application of the Transfer Matrix Method to Anti-reflective Coating Rendering. In *Advances in Computer Graphics: 37th Computer Graphics International Conference, CGI 2020, Geneva, Switzerland, October 20–23, 2020, Proceedings* (Geneva, Switzerland). Springer-Verlag, Berlin, Heidelberg, 83–95. doi:10.1007/978-3-030-61864-3_8

[4] Jay S. Gondek, Gary W. Meyer, and Jonathan G. Newman. 1994. Wavelength dependent reflectance functions. In *Proceedings of the 21st Annual Conference on Computer Graphics and Interactive Techniques (SIGGRAPH '94)*. Association for Computing Machinery, New York, NY, USA, 213–220. doi:10.1145/192161.192202

[5] Hideki Hirayama, Kazufumi Kaneda, Hideo Yamashita, and Yoshimi Monden. 2001. An accurate illumination model for objects coated with multilayer films. *Computers & Graphics* 25, 3 (2001), 391–400. doi:10.1016/S0097-8493(01)00063-2

[6] Michael Hurben. 2024. Anti-Reflection Coatings Part II: The Transfer Matrix Method. Retrieved April 16, 2025 from https://legallyblindbirding.net/2024/12/14/anti-reflection-coatings-part-ii-the-transfer-matrix-method/

[7] Claudio Oton. 2022. Multilayer calculator with transfer-matrix method. Retrieved April 16, 2025 from https://andtherewaslight.github.io/multilayer/

[8] Ken Perlin. 1985. An image synthesizer. In *Proceedings of the 12th Annual Conference on Computer Graphics and Interactive Techniques (SIGGRAPH '85)*. Association for Computing Machinery, New York, NY, USA, 287–296. doi:10.1145/325334.325247

[9] Fu-kun Wu and Chang-wen Zheng. 2015. Microfacet-based interference simulation for multilayer films. *Graph. Models* 78, C (March 2015), 26–35. doi:10.1016/j.gmod.2014.12.003